

# Quantum Walk-based Generation of Entanglement Between Two Walkers

Salvador E. Venegas-Andraca<sup>1</sup> and Sougato Bose<sup>2</sup>

<sup>1</sup>*Quantum Information Processing Group, Tecnológico de Monterrey Campus Estado de México, Carretera Lago Gpe. Km 3.5, Atizapán de Zaragoza, Edo. México, 52926, México  
sva@mindsfomexico.org, salvador.venegas-andraca@keble.oxon.org*

<sup>2</sup>*Department of Physics and Astronomy, University College of London. Gower Street, London WC1E 6BT, United Kingdom  
sougato@theory.phys.ucl.ac.uk*

Quantum walks can be used either as tools for quantum algorithm development or as entanglement generators, potentially useful to test quantum hardware. We present a novel algorithm based on a discrete Hadamard quantum walk on a line with one coin and two walkers whose purpose is to generate entanglement between walkers. We provide several classical computer simulations of our quantum algorithm in which we show that, although the asymptotical amount of entanglement generated between walkers does not reach the highest degree of entanglement possible at each step for either coin measurement outcome, the entanglement ratio (entanglement generated/highest value of entanglement possible, for each step) tends to converge, and the actual convergence value depends on the coin initial state and on the coin measurement outcome. Furthermore, our numerical simulations show that, for the quantum walks used in our algorithm, the value towards which entanglement ratio converges also depends on the position probability distribution symmetry of a quantum walk computed with one single walker and the same coin initial state employed in the corresponding quantum walk with two walkers.

PACS numbers: PACS numbers: 03.67.Bg, 03.67.Lx, 03.67.-a, 03.67.Ac

## I. INTRODUCTION

Quantum walks were designed as quantum counterparts of classical random walks, a branch of stochastic processes widely used in algorithm development. Although some authors have selected the name “quantum random walk” to refer to quantum phenomena [1, 2, 3] and, in fact, in the seminal work by R.P. Feynman [4] about quantum mechanical computers we find a proposal that could be interpreted as a (continuous-time) quantum walk [5], it is generally accepted that the first paper with quantum walks as its main topic was published in 1993 by Aharonov *et al* [6]. Thus, the links between classical random walks and quantum walks, as well as the utility of quantum walks in computer science, are two fresh and open areas of research.

Since one of the main goals in quantum computing is the development of quantum algorithms, and given the success of employing classical random walks for computing solutions to NP-complete problems [7, 8, 9], there has been a huge interest in understanding the physical and computational properties of quantum walks over the last few years on both experimental [10, 11, 12, 13, 14] and theoretical research communities (see [15] for a review on theoretical aspects of quantum walks). In addition to their usage in computer science, the study of quantum walks is relevant to the modelling of physical phenomena such as energy transfer in photosynthetic systems [16]. Moreover, although it has been proved that certain properties of quantum walks are also reproducible by classical systems (like variance enhancement with respect to classical random walks [17, 18, 19]), it is also true that uniquely quantum mechanical properties of quantum walks, such as entanglement, may be employed to

building methods in order to test the “quantumness” of emerging technologies for the creation of quantum computers. Thus it is of crucial importance to develop methods of entanglement generation through quantum walks so that the genuine quantum nature of a given walk with given physical systems may be tested.

Quantum entanglement has been incorporated into quantum walks research either as a result of performing a quantum walk [20, 21, 22, 23, 24, 25] or as a resource to build new kinds of quantum walks [26, 27, 28, 29]. Since entanglement is a key component in quantum computation, it is worth keeping in mind that quantum walks can be used either as entanglement generators or as computational processes taking advantage of this quantum mechanical property.

In this paper we introduce a novel algorithm based on a discrete quantum walk on a line with one coin and two walkers whose purpose is to generate entanglement between walkers. After evolving the quantum walk for a certain number of steps, we perform a measurement on the coin state. We then obtain a post-measurement quantum state composed by the tensor product of one coin state and several walker components. We take the walker components of this post-measurement state and calculate the entanglement between walkers. We perform many quantum walks with the same initial conditions and evolution operators, so that we have a quantum walk ready to be measured for each time step. In addition to our algorithm, we provide several simulation results using different initial conditions for the proposed quantum walks. While this analysis highlights the potential of a quantum walk to entangle high dimensional quantum systems (the dimension of the space available to the walkers grow in each step) it can also at times be

practically useful. This will be the case when the walkers are systems which do not directly interact with each other such as two different electromagnetic field modes. Then the coin can be a common system such as an atom which interact with both and can entangle them to a high degree with the degree depending on the number of steps possible within the reasonable decoherence time of the fields.

## II. ALGORITHM FOR ENTANGLEMENT GENERATION

In this section we present our algorithm for the generation of entanglement in a family of quantum walks on an unrestricted line. A succinct mathematical representation of a quantum walk after  $n$  steps is

$$|\psi\rangle_n = (\hat{U})^n |\psi\rangle_{\text{initial}}, \quad (1)$$

where  $|\psi\rangle_{\text{initial}}$  is the initial total state of the quantum walk. In our case, the family of quantum walks we shall employ is composed by the tensor product of one coin and two walkers

$$|\text{coin}\rangle \otimes |\text{walker}_1, \text{walker}_2\rangle \quad (2)$$

as total initial state. After several applications of an evolution operator composed of a coin operator and a shift operator, we perform a measurement on the coin state. The result of this operation is a post-measurement quantum state composed by the tensor product of one coin state and several walker components. We take the walker components of this coin post-measurement state and calculate the entanglement between walkers using the von Neumann entropy

$$E(|\psi\rangle) = S(\rho_A) = S(\rho_B) = - \sum_{i=1}^d \alpha_i^2 \log_2(\alpha_i^2). \quad (3)$$

where  $|\psi\rangle = \sum_{i=1}^d \alpha_i |i_A\rangle |i_B\rangle$  is the Schmidt decomposition of a bipartite quantum state  $|\psi\rangle$ . We compute  $n$  quantum walks using the same initial states and evolution operator in order to measure the degree of entanglement between walkers *for each step*, so that the final result of this algorithm is a graph with the amount of entanglement available at each step. We summarize this explanation in algorithm 1.

### Algorithm 1. Quantification of entanglement.

Input: A maximum number of steps  $n$  for the quantum walk, and  $n$  identically prepared total initial states  $|\psi\rangle_0$  with one coin and two walkers.

Objective: To quantify the amount of entanglement between walkers for each step of the quantum walk.

01. Set  $t=1$

02. While ( $t \leq n$ )

03. Apply the evolution operator  $\hat{U}^t = (\hat{S}(\hat{C} \otimes \hat{I}))^t$  to  $|\psi\rangle_0$ .

04. Perform a measurement on the coin system. Since  $|\text{coin}\rangle \in \mathcal{H}^2$  there are only two possible outcomes. We label them  $\alpha_0$  and  $\alpha_1$ .

05. For outcome  $\alpha_0$  then

06. Compute the post-measurement quantum state  $|\psi\rangle_{t,pm}^{c_0}$

07. Quantify entanglement between walkers from quantum state  $|\psi\rangle_{t,pm}^{c_0}$

08. For outcome  $\alpha_1$  then

09. Compute the post-measurement quantum state  $|\psi\rangle_{t,pm}^{c_1}$

10. Quantify entanglement between walkers from quantum state  $|\psi\rangle_{t,pm}^{c_1}$

11. Increase  $t$  by 1

As stated in the introduction, we are interested in quantifying the amount of entanglement between walkers for each coin outcome, as well as in studying the impact of different initial quantum states in this quantification of entanglement. The following lines shows corresponding results using unrestricted quantum walks on a line.

### A. Entanglement Generation in unrestricted Quantum Walks on a Line

We shall use Eqs. (4a)-(4e) as total initial states, where each initial condition has the form  $|\psi\rangle_0 = |\text{coin}\rangle_0 \otimes |\text{position}\rangle_0$ , with  $|\text{coin}\rangle_0$  as coin initial state and  $|\text{position}\rangle_0$  as walker initial state.

$$|\psi\rangle_0 = |0\rangle_c \otimes |0,0\rangle_p \quad (4a)$$

$$|\psi\rangle_0 = |1\rangle_c \otimes |0,0\rangle_p \quad (4b)$$

$$|\psi\rangle_0 = \left(\frac{1}{\sqrt{2}}|0\rangle_c + \frac{i}{\sqrt{2}}|1\rangle_c\right) \otimes |0,0\rangle_p \quad (4c)$$

$$|\psi\rangle_0 = \left(\frac{i}{\sqrt{2}}|0\rangle_c + \frac{1}{\sqrt{2}}|1\rangle_c\right) \otimes |0,0\rangle_p \quad (4d)$$

$$|\psi\rangle_0 = (\sqrt{0.85}|0\rangle_c - \sqrt{0.15}|1\rangle_c) \otimes |0,0\rangle_p \quad (4e)$$

where subindex  $c$  stands for ‘coin’ and subindex  $p$  stands for ‘walker position’.

Additionally, we use the Hadamard operator as coin operator

$$\hat{H} = \frac{1}{\sqrt{2}}(|0\rangle_c \langle 0| + |0\rangle_c \langle 1| + |1\rangle_c \langle 0| - |1\rangle_c \langle 1|) \quad (5)$$

Our shift operator is given by

$$\hat{S}_{\text{ent}} = |0\rangle_c \langle 0| \otimes \sum_i |i+1, i+1\rangle_p \langle i, i| + |1\rangle_c \langle 1| \otimes \sum_i |i-1, i-1\rangle_p \langle i, i| \quad (6)$$

The observable used for coin measurement (step 4 of algorithm 1) is given by

$$\hat{M} = \alpha_0 \hat{M}_0 + \alpha_1 \hat{M}_1 = \alpha_0 |0\rangle_c \langle 0| + \alpha_1 |1\rangle_c \langle 1| \quad (7)$$

With the purpose of exemplifying the behavior of algorithm 1, we show in the following lines three steps of a quantum walk and corresponding entanglement measurement using Eq. (4a) as total initial state, and Eqs. (5) and (6) as corresponding coin and shift operators. Using Eq. (1) we find that

$$|\psi\rangle_1 = \frac{1}{\sqrt{2}} (|0\rangle_c |1, 1\rangle_p + |1\rangle_c |-1, -1\rangle_p) \quad (8)$$

$$|\psi\rangle_2 = \frac{1}{2} (|0\rangle_c |2, 2\rangle_p + |1\rangle_c |0, 0\rangle_p + |0\rangle_c |0, 0\rangle_p - |1\rangle_c |-2, -2\rangle_p) \quad (9)$$

$$|\psi\rangle_3 = \frac{1}{2\sqrt{2}} (|0\rangle_c |3, 3\rangle_p + |1\rangle_c |1, 1\rangle_p + |0\rangle_c |1, 1\rangle_p - |1\rangle_c |-1, -1\rangle_p + |0\rangle_c |1, 1\rangle_p + |1\rangle_c |-1, -1\rangle_p - |0\rangle_c |-1, -1\rangle_p + |1\rangle_c |-3, -3\rangle_p) \quad (10)$$

For  $|\psi\rangle_1$  (Eq. (8)), the post-measurement quantum state after performing a coin measurement with measurement operator  $\hat{M}_0$  (Eq. (7)) is given by  $|\psi\rangle_{1,pm}^{c_0} = |0\rangle_c |1, 1\rangle_p$ , and the degree of entanglement between walkers is clearly 0. As for coin 1, we perform a coin measurement on  $|\psi\rangle_1$  (Eq. (8)) using measurement operator  $\hat{M}_1$  (Eq. (7)), obtaining as post-measurement quantum state  $|\psi\rangle_{1,pm}^{c_1} = |1\rangle_c |-1, -1\rangle_p$ . It is also clear that the degree of entanglement between walkers in  $|\psi\rangle_{1,pm}^{c_1}$  is 0.

In step 2 (Eq. (9)), we have  $|\psi\rangle_{2,pm}^{c_0} = \frac{1}{\sqrt{2}} |0\rangle_c (|2, 2\rangle_p + |0, 0\rangle_p)$  as coin  $|0\rangle_c$  post-measurement state, and corresponding entanglement between walkers is equal to 1, since  $\frac{1}{\sqrt{2}} (|2, 2\rangle_p + |0, 0\rangle_p)$  is a maximally entangled state. Along the same lines, the coin  $|1\rangle_c$  post-measurement state is given by  $|\psi\rangle_{2,pm}^{c_1} = \frac{1}{\sqrt{2}} (|1\rangle_c (|0, 0\rangle_p + |-2, -2\rangle_p))$ . Since  $\frac{1}{\sqrt{2}} (|0, 0\rangle_p + |-2, -2\rangle_p)$  is a maximally entangled state, its degree of entanglement is equal to 1.

Finally, in step 3 (Eq. (10)),  $|\psi\rangle_{3,pm}^{c_0} = \frac{1}{\sqrt{6}} |0\rangle_c (|3, 3\rangle_p + 2|1, 1\rangle_p - |-1, -1\rangle_p)$ , and corresponding degree of entanglement between walkers is equal to 1.2516 (maximum degree of entanglement attainable between walkers is  $\log_2 3 = 1.585$ .) As for coin  $|1\rangle_c$ ,  $|\psi\rangle_{3,pm}^{c_1} =$

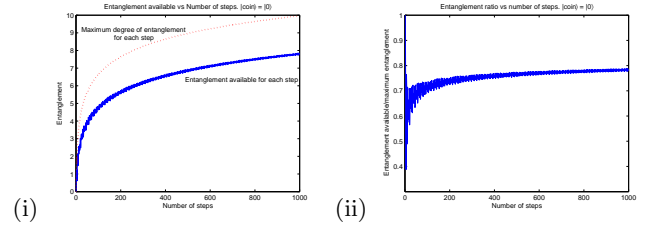


FIG. 1: After computing a 1000-steps quantum walk  $|\psi\rangle_{1000} = [\hat{S}_{\text{ent}}(\hat{H} \otimes \hat{I})]^{1000} |\psi\rangle_0$  with  $|\psi\rangle_0$  given by Eq. (4a) and Eqs. (5) and (6) as coin ( $\hat{H}$ ) and shift ( $\hat{S}$ ) operators, we perform a coin measurement on  $|\psi\rangle_{1000}$  using measurement operator  $\hat{M}_0$  (Eq. (7)). The thin line of (i) (red color online) shows the maximum degree of entanglement between walkers attainable in the post-measurement quantum state  $|\psi\rangle_{t,pm}^{c_0}$  (for example,  $\log_2 2 = 1$  for the second step and  $\log_2 3 = 1.585$  for the third step), and the thick line of (i) (blue color online) shows the actual entanglement between walkers available at each step. We can see that, asymptotically, the entanglement available is about 80% of the corresponding maximum degree of entanglement (plot (ii)).

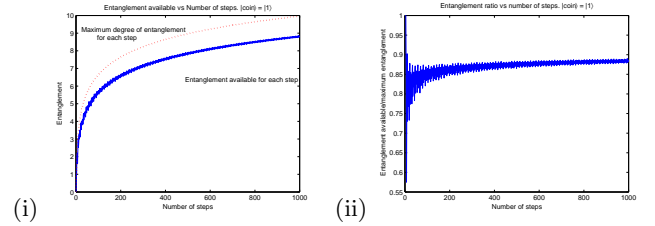


FIG. 2: After computing of a 1000-steps quantum walk  $|\psi\rangle_{1000} = [\hat{S}_{\text{ent}}(\hat{H} \otimes \hat{I})]^{1000} |\psi\rangle_0$  with  $|\psi\rangle_0$  given by Eq. (4a) and Eqs. (5) and (6) as coin ( $\hat{H}$ ) and shift ( $\hat{S}$ ) operators, we perform a coin measurement on  $|\psi\rangle_{1000}$  using measurement operator  $\hat{M}_1$  (Eq. (7)). The thin curve of (i) (red color online) shows the maximum degree of entanglement between walkers attainable in the post-measurement quantum state  $|\psi\rangle_{t,pm}^{c_1}$  (for example,  $\log_2 2 = 1$  for the second step and  $\log_2 3 = 1.585$  for the third step), and the thick curve of (i) (blue color online) shows the actual entanglement between walkers available at each step. We can see that, for large number of steps, the entanglement available is about 90% of the corresponding maximum degree of entanglement (graph (ii)).

$\frac{1}{\sqrt{2}} (|0\rangle_c (|1, 1\rangle_p + |-3, -3\rangle_p))$ , with degree of entanglement between walkers equal to 1.

We show in Figs. (1), (2) and (3), simulation results for a 1000-steps quantum walk performed with Eq. (4a) as total initial state and Eqs. (5) and (6) as coin and shift operators.

Fig. (1) presents the results of measuring entanglement between walkers in a coin  $|0\rangle_c$  post-measurement state  $|\psi\rangle_{t,pm}^{c_0}$ . In Fig. (1.i) we show two curves. The thin curve (red color online) indicates, for each step of the quantum walk, the maximum amount of entanglement between walkers achievable at each time step, while the thick curve (blue color online) shows the actual degree

of entanglement between walkers available for each step. We can see that, as the number of steps increases, the amount of entanglement available vs the maximum degree of entanglement attainable is about 80% (Figure (1.ii).)

In Fig. (2) we present the same results as in Fig. (1) but for a coin  $|1\rangle_c$  post-measurement state  $|\psi\rangle_{t,pm}^{c1}$ . First of all, we notice that, as in the previous paragraph, the degree of entanglement between walkers available in  $|\psi\rangle_{t,pm}^{c1}$  (thin line (red color online) of Fig. (2.i)) does not reach the highest degree of entanglement attainable at each time step (thick (blue color online) line in Fig. (2.i)). However, it can be seen by comparing the asymptotical behavior shown in Fig. (1.i) and Fig. (2.i) that, if the coin measurement outcome is  $\alpha_1$  (Fig. (2.i)) then the amount of entanglement available between walkers tends to be higher (about 90%, Fig. (2.ii)) than the corresponding degree of entanglement between walkers for a coin measurement outcome  $\alpha_0$  (Fig. (1.i)) which is, as shown in Fig. (1.ii), about 80%.

In Fig. (3.i) we display the probability vs location graph of a 1000-step Hadamard quantum walk with an initial state given by  $|0\rangle_c \otimes |0\rangle_p$  (i.e. one coin and only one walker) and shift operator provided by

$$\hat{S} = |0\rangle_c \langle 0| \otimes \sum_i |i+1\rangle_p \langle i| + |1\rangle_c \langle 1| \otimes \sum_i |i-1\rangle_p \langle i|. \quad (11)$$

The symmetry of this walk, about a line passing through the origin and perpendicular to the  $x$  axis, is the same as that of a Hadamard quantum walk with initial state given by  $|\psi\rangle = |0\rangle_c \otimes |0,0\rangle_p$  and shift operator given by Eq. (6). The black curve of Fig. (3.ii) shows the amount of entanglement available between walkers in the post-measurement state  $|\psi\rangle_{t,pm}^{c0}$  (as in Fig. (1.i)), while the gray curve (red color online) shows the corresponding degree of entanglement available between walkers for post-measurement state  $|\psi\rangle_{t,pm}^{c1}$  (as in Fig. (2.i)). The purpose of Fig. (3) is to relate the amount of entanglement available for each coin post-measurement state with the symmetry of the quantum walk and, consequently, with the total initial state of the quantum walk. We shall come back to Fig. (3) shortly.

We now focus on Figs. (4), (5) and (6), which present the numerical behavior of a quantum walk with initial quantum state given by Eq. (4b), and Eqs. (5) and (6) as coin and shift operators, respectively.

As in the previous case, Figs. (4) and (5) display the results of measuring entanglement between walkers in a coin  $|0\rangle_c$  post-measurement state  $|\psi\rangle_{t,pm}^{c0}$  and a coin  $|1\rangle_c$  post-measurement state  $|\psi\rangle_{t,pm}^{c1}$ . However, and in contrast to Figs. (1)-(3), in this case we see that, as the number of steps increases, *the entanglement between walkers for  $|\psi\rangle_{t,pm}^{c0}$  (about 90% with respect to the degree of entanglement attainable in each step, Fig. (4.ii)) is higher than that of state  $|\psi\rangle_{t,pm}^{c1}$  (about 80% with respect to the degree of entanglement attainable in each step, Fig. (5.ii))*. As we can see by comparing Figs. (3) and (6),

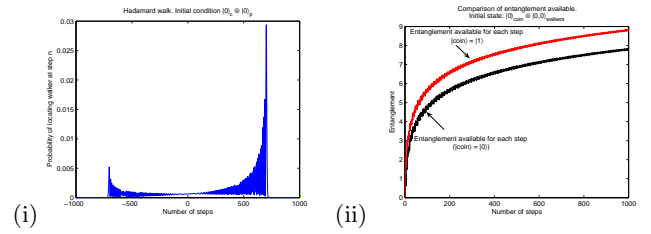


FIG. 3: Plot (i) presents the probability vs location graph of a 1000-step Hadamard quantum walk with an initial state  $|0\rangle_c \otimes |0\rangle_p$  and shift operator provided by Eq. (11). The symmetry of this walk, about a line passing through the origin and perpendicular to the  $x$  axis, is the same as that of a Hadamard quantum walk with initial state given by  $|\psi\rangle = |0\rangle_c \otimes |0,0\rangle_p$  and shift operator given by Eq. (6). Plot (ii) is a summary of Figs. (1.i) and (2.i), and shows that the amount of entanglement between walkers available in post-measurement state  $|\psi\rangle_{t,pm}^{c1}$  tends to be higher than the amount of entanglement between walkers available in post-measurement state  $|\psi\rangle_{t,pm}^{c0}$ .

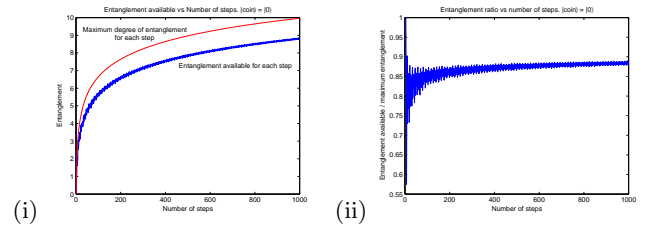


FIG. 4: Entanglement values for coin post-measurement state  $|\psi\rangle_{t,pm}^{c0}$  computed from a 1000-steps quantum walk  $|\psi\rangle_{1000} = [\hat{S}_{ent}(\hat{H} \otimes \hat{I})]^{1000} |\psi\rangle_0$  with  $|\psi\rangle_0$  given by Eq. (4b), Eqs. (5) and (6) as coin ( $\hat{H}$ ) and shift ( $\hat{S}$ ) operators, and measurement operator  $\hat{M}_0$  (Eq. (7)). The thin line of (i) (red color online) shows the maximum degree of entanglement between walkers attainable in the post-measurement quantum state  $|\psi\rangle_{t,pm}^{c0}$ , and the thick line of (i) (blue color online) shows the actual entanglement between walkers available at each step. We can see that, asymptotically, the entanglement available is about 90% of the corresponding maximum degree of entanglement (plot (ii)). Note that this amount of entanglement available between walkers (90%) is *higher* than the amount of entanglement available between walkers (80%) for coin  $|0\rangle_c$  post-measurement quantum state with initial state  $|0\rangle_c \otimes |0,0\rangle_p$  (Fig. (1)).

the symmetry of the probability distribution computed with initial quantum state given by Eq. (4b) (Fig. (6.i)) seems to have a significant effect on the actual entanglement values for  $|\psi\rangle_{t,pm}^{c0}$  and  $|\psi\rangle_{t,pm}^{c1}$ .

So, a natural step forward is to compute quantum walks with initial states that produce symmetric probability distributions, in order to see the asymptotical behavior of entanglement. With this thought in mind we have computed the following three sets of numerical simulations.

The first set consists of Figs. (7), (8) and (9), in which we expose the numerical behavior of a quantum walk with initial quantum state given by Eq. (4c), i.e.

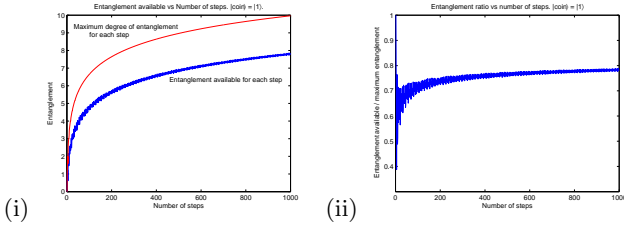


FIG. 5: Entanglement values for coin post-measurement state  $|\psi\rangle_{t,pm}^{c_1}$  computed from a 1000-steps quantum walk  $|\psi\rangle_{1000} = [\hat{S}_{ent}(\hat{H} \otimes \hat{I})]^{1000}|\psi\rangle_0$  with  $|\psi\rangle_0$  given by Eq. (4b), Eqs. (5) and (6) as coin ( $\hat{H}$ ) and shift ( $\hat{S}$ ) operators, and measurement operator  $\hat{M}_1$  (Eq. (7)). The thin line of (i) (red color online) shows the maximum degree of entanglement between walkers attainable in the post-measurement quantum state  $|\psi\rangle_{t,pm}^{c_1}$ , and the thick line of (i) (blue color online) shows the actual entanglement between walkers available at each step. We can see that, asymptotically, the entanglement available is about 80% of the corresponding maximum degree of entanglement (plot (ii)). Note that this amount of entanglement available between walkers (80%) is *less* than the amount of entanglement available between walkers (90%) for coin  $|1\rangle_c$  post-measurement quantum state with initial state  $|0\rangle_c \otimes |0,0\rangle_p$  (Fig. (2)).

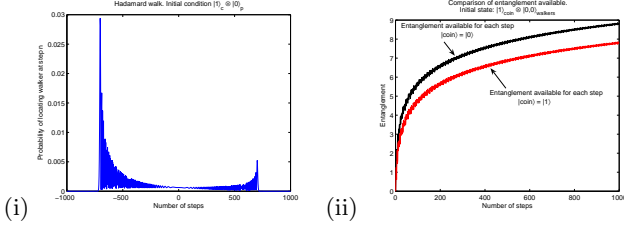


FIG. 6: Plot (i) presents the probability vs location graph of a 1000-step Hadamard quantum walk with an initial state  $|1\rangle_c \otimes |0\rangle_p$  and shift operator provided by Eq. (11). The symmetry of this walk, about a line passing through the origin and perpendicular to the  $x$  axis, is the same as that of a Hadamard quantum walk with initial state given by  $|\psi\rangle = |1\rangle_c \otimes |0,0\rangle_p$  (Eq. (4b)) and shift operator given by Eq. (6). Plot (ii) is a summary of Figs. (4.i) and (5.i), and shows that the amount of entanglement between walkers available in post-measurement state  $|\psi\rangle_{t,pm}^{c_1}$  tends to be *less* than the amount of entanglement between walkers available in post-measurement state  $|\psi\rangle_{t,pm}^{c_0}$ , in stark contrast to the numerical results computed for a quantum walk with total initial state  $|0\rangle_c \otimes |0,0\rangle_p$  (Figs. (1-3)).

$|\psi\rangle_0 = (\frac{1}{\sqrt{2}}|0\rangle_c + \frac{i}{\sqrt{2}}|1\rangle_c) \otimes |0,0\rangle_p$ , and Eqs. (5) and (6) as coin and shift operators, respectively. Fig. (7) shows the results of measuring entanglement between walkers in a coin  $|0\rangle_c$  post-measurement state  $|\psi\rangle_{t,pm}^{c_0}$ , while Fig. (8) introduces corresponding results for a coin  $|1\rangle_c$  post-measurement state  $|\psi\rangle_{t,pm}^{c_1}$ .

Although an initial quantum state of the form given by Eq. (4c) produces a balanced probability distribution (Fig. (9.i)), such a property does not have a significant effect on the degree of entanglement between walkers (Fig. (9.ii)). In fact, comparing plots from Figs. (3.ii) and

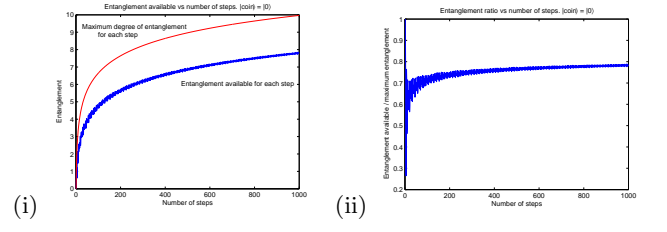


FIG. 7: Entanglement values for coin  $|0\rangle_c$  post-measurement state  $|\psi\rangle_{t,pm}^{c_0}$  computed from a 1000-steps quantum walk  $|\psi\rangle_{1000} = [\hat{S}_{ent}(\hat{H} \otimes \hat{I})]^{1000}|\psi\rangle_0$  with  $|\psi\rangle_0 = (\frac{1}{\sqrt{2}}|0\rangle_c + \frac{i}{\sqrt{2}}|1\rangle_c) \otimes |0,0\rangle_p$  given by Eq. (4c), coin ( $\hat{H}$ ) and shift ( $\hat{S}$ ) operators given by Eqs. (5) and (6) respectively, and measurement operator  $\hat{M}_0$  (Eq. (7)). The thin line of (i) (red color online) shows the maximum degree of entanglement between walkers attainable in the post-measurement quantum state  $|\psi\rangle_{t,pm}^{c_0}$ , and the thick line of (i) (blue color online) shows the actual entanglement between walkers available at each step. The asymptotical behavior of entanglement values for this quantum walk is the same as that shown by a quantum walk with total initial state  $|0\rangle_c \otimes |0,0\rangle_p$  (Fig. (1)).

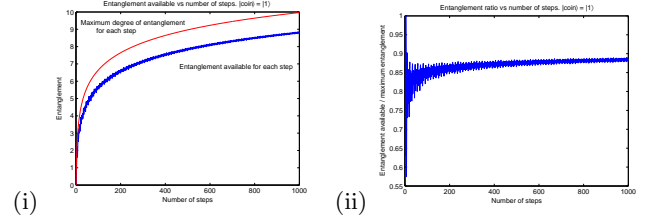


FIG. 8: Entanglement values for coin  $|1\rangle_c$  post-measurement state  $|\psi\rangle_{t,pm}^{c_1}$  computed from a 1000-steps quantum walk  $|\psi\rangle_{1000} = [\hat{S}_{ent}(\hat{H} \otimes \hat{I})]^{1000}|\psi\rangle_0$  with  $|\psi\rangle_0 = (\frac{1}{\sqrt{2}}|0\rangle_c + \frac{i}{\sqrt{2}}|1\rangle_c) \otimes |0,0\rangle_p$  given by Eq. (4c), coin ( $\hat{H}$ ) and shift ( $\hat{S}$ ) operators given by Eqs. (5) and (6) respectively, and measurement operator  $\hat{M}_1$  (Eq. (7)). The thin line of (i) (red color online) shows the maximum degree of entanglement between walkers attainable in the post-measurement quantum state  $|\psi\rangle_{t,pm}^{c_1}$ , and the thick line of (i) (blue color online) shows the actual entanglement between walkers available at each step. The asymptotical behavior of entanglement values for this quantum walk is the same as that shown by a quantum walk with total initial state  $|0\rangle_c \otimes |0,0\rangle_p$  (Fig. (2)).

(9.ii) shows that the asymptotical behavior of entanglement values for a quantum walk with initial state given by Eq. (4a) is the same as those entanglement values computed for a quantum walk with initial state given by Eq. (4c).

Figs. (10) - (12) introduce the asymptotics of entanglement values for a quantum walk with initial state given by Eq. (4d). Again, although the initial state  $|\psi\rangle_0 = (\frac{i}{\sqrt{2}}|0\rangle_c + \frac{1}{\sqrt{2}}|1\rangle_c) \otimes |0,0\rangle_p$  produces a symmetrical probability distribution (Fig. (12.i)), we notice that the asymptotical behavior of entanglement values for a coin  $|0\rangle_c$  post-measurement quantum state  $|\psi\rangle_{t,pm}^{c_0}$  is different from that of a coin  $|1\rangle_c$  post-measurement quantum



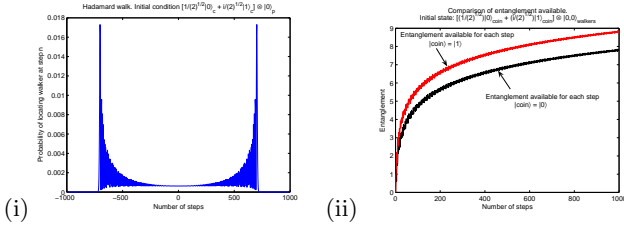


FIG. 9: Plot (i) presents the probability vs location graph of a 1000-step Hadamard quantum walk with an initial state  $(\frac{1}{\sqrt{2}}|0\rangle_c + \frac{i}{\sqrt{2}}|1\rangle_c) \otimes |0\rangle_p$  and shift operator provided by Eq. (11). The symmetry of the probability distribution shown in plot (i) is the same as that of a Hadamard quantum walk with initial state given by  $|\psi\rangle_0 = (\frac{1}{\sqrt{2}}|0\rangle_c + \frac{i}{\sqrt{2}}|1\rangle_c) \otimes |0, 0\rangle_p$  and shift operator given by Eq. (6). Although the symmetry of plot (i) is significantly different from that of Fig. (3.i), plot (ii) shows the same asymptotical behavior as that of Fig. (3.ii).

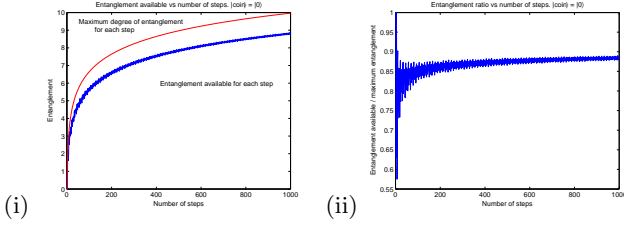


FIG. 10: Entanglement values for coin  $|0\rangle_c$  post-measurement state  $|\psi\rangle_{t,pm}^{c0}$  computed from a 1000-steps quantum walk  $|\psi\rangle_{1000} = [\hat{S}_{ent}(\hat{H} \otimes \hat{I})]^{1000}|\psi\rangle_0$  with  $|\psi\rangle_0 = (\frac{i}{\sqrt{2}}|0\rangle_c + \frac{1}{\sqrt{2}}|1\rangle_c) \otimes |0, 0\rangle_p$  given by Eq. (4d), coin  $(\hat{H})$  and shift  $(\hat{S})$  operators given by Eqs. (5) and (6) respectively, and measurement operator  $\hat{M}_0$  (Eq. (7)). The thin line of (i) (red color online) shows the maximum degree of entanglement between walkers attainable in the post-measurement quantum state  $|\psi\rangle_{t,pm}^{c0}$ , and the thick line of (i) (blue color online) shows the actual entanglement between walkers available at each step. The asymptotical behavior of entanglement values for this quantum walk is the same as that shown by a quantum walk with total initial state  $|1\rangle_c \otimes |0, 0\rangle_p$  (Fig. (4)).

state  $|\psi\rangle_{t,pm}^{c1}$  (Fig. (12.ii)). In fact, comparing plots from Figs. (4) and (10) for a coin  $|0\rangle$  post-measurement quantum state  $|\psi\rangle_{t,pm}^{c0}$ , and plots from Figs. (5) and (11) for a coin  $|1\rangle$  post-measurement quantum state  $|\psi\rangle_{t,pm}^{c1}$ , shows that the asymptotics of entanglement values for initial states given by Eqs. (4b) and (4d) are the same.

However and in stark contrast to the previous cases, the symmetry properties of the probability distribution of a quantum walk with initial state  $|\psi\rangle_0 = (\sqrt{0.85}|0\rangle_c - \sqrt{0.15}|1\rangle_c) \otimes |0, 0\rangle_p$  (Eq. (4e)) does have an effect of the entanglement between walkers produced from coin post-measurement quantum states.

In Figs. (13) and (14) we exhibit the asymptotical behavior of entanglement values of coin post-measurement states  $|\psi\rangle_{t,pm}^{c0}$  and  $|\psi\rangle_{t,pm}^{c1}$  respectively, for a quantum walk with initial state given by Eq. (4e). As op-

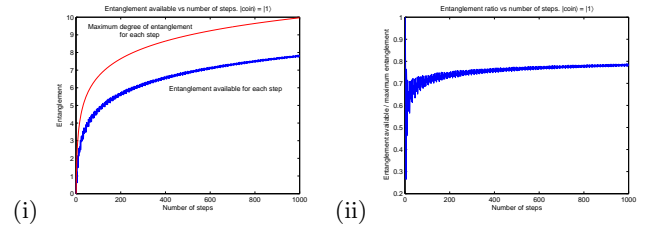


FIG. 11: Entanglement values for coin  $|1\rangle_c$  post-measurement state  $|\psi\rangle_{t,pm}^{c1}$  computed from a 1000-steps quantum walk  $|\psi\rangle_{1000} = [\hat{S}_{ent}(\hat{H} \otimes \hat{I})]^{1000}|\psi\rangle_0$  with  $|\psi\rangle_0 = (\frac{i}{\sqrt{2}}|0\rangle_c + \frac{1}{\sqrt{2}}|1\rangle_c) \otimes |0, 0\rangle_p$  given by Eq. (4d), coin  $(\hat{H})$  and shift  $(\hat{S})$  operators given by Eqs. (5) and (6) respectively, and measurement operator  $\hat{M}_1$  (Eq. (7)). The thin line of (i) (red color online) shows the maximum degree of entanglement between walkers attainable in the post-measurement quantum state  $|\psi\rangle_{t,pm}^{c1}$ , and the thick line of (i) (blue color online) shows the actual entanglement between walkers available at each step. The asymptotical behavior of entanglement values for this quantum walk is the same as that shown by a quantum walk with total initial state  $|1\rangle_c \otimes |0, 0\rangle_p$  (Fig. (5)).

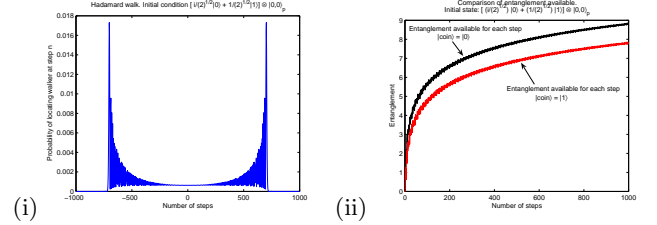


FIG. 12: Plot (i) presents the probability vs location graph of a 1000-step Hadamard quantum walk with an initial state  $(\frac{i}{\sqrt{2}}|0\rangle_c + \frac{1}{\sqrt{2}}|1\rangle_c) \otimes |0\rangle_p$  and shift operator provided by Eq. (11). The symmetry of the probability distribution shown in plot (i) is the same as that of a Hadamard quantum walk with initial state given by  $|\psi\rangle = (\frac{i}{\sqrt{2}}|0\rangle_c + \frac{1}{\sqrt{2}}|1\rangle_c) \otimes |0, 0\rangle_p$  and shift operator given by Eq. (6). Although the symmetry of plot (i) is significantly different from that of Fig. (6.i), plot (ii) shows the same asymptotical behavior as that of Fig. (6.ii).

posed to previous cases in which asymptotical values of entanglement between walkers were different for post-measurement states  $|\psi\rangle_{t,pm}^{c0}$  and  $|\psi\rangle_{t,pm}^{c1}$ , we can see in Figs. (13) and (14) that the asymptotics of both entanglement curves tend to the same efficiency of 85% approximately. This tendency can also be seen in Fig. (15.ii) where we show that both entanglement curves overlap.

### III. CONCLUSIONS

We have proposed an algorithm to generate entanglement between walkers, after measuring the coin state, for a Hadamard quantum walk with one (2-dimensional) coin and two walkers. Our numerical simulations show that, asymptotically, the amount of entanglement generated between walkers does not reach the highest degree

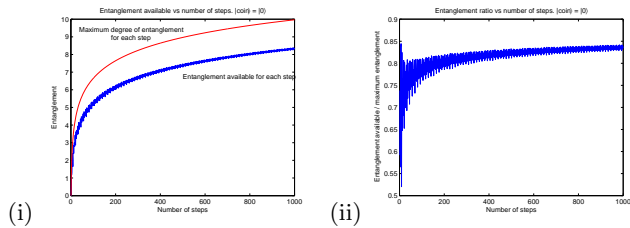


FIG. 13: Entanglement values for coin  $|0\rangle_c$  post-measurement state  $|\psi\rangle_{t,pm}^{c_0}$  computed from a 1000-steps quantum walk  $|\psi\rangle_{1000} = [\hat{S}_{ent}(\hat{H} \otimes \hat{I})]^{1000}|\psi\rangle_0$  with  $|\psi\rangle_0 = (\sqrt{0.85}|0\rangle_c - \sqrt{0.15}|1\rangle_c) \otimes |0, 0\rangle_p$  given by Eq. (4e), coin ( $\hat{H}$ ) and shift ( $\hat{S}$ ) operators given by Eqs. (5) and (6) respectively, and measurement operator  $\hat{M}_0$  (Eq. (7)). The thin line of (i) (red color online) shows the maximum degree of entanglement between walkers attainable in the post-measurement quantum state  $|\psi\rangle_{t,pm}^{c_0}$ , and the thick line of (i) (blue color online) shows the actual entanglement between walkers available at each step. We can see that the asymptotics of entanglement values given in plot (ii) tend to the same values as those shown in Fig. (14), obtained from a coin  $|1\rangle_c$  post-measurement state  $|\psi\rangle_{t,pm}^{c_1}$  computed from a quantum walk with the same initial state (Eq. (4e)).

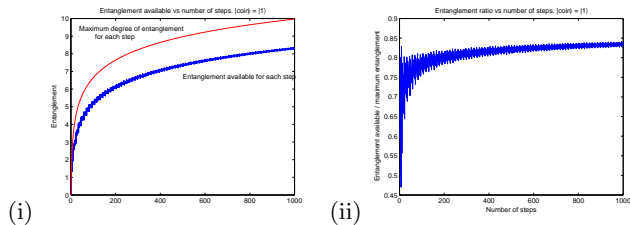


FIG. 14: Entanglement values for coin  $|1\rangle_c$  post-measurement state  $|\psi\rangle_{t,pm}^{c_1}$  computed from a 1000-steps quantum walk  $|\psi\rangle_{1000} = [\hat{S}_{ent}(\hat{H} \otimes \hat{I})]^{1000}|\psi\rangle_0$  with  $|\psi\rangle_0 = (\sqrt{0.85}|0\rangle_c - \sqrt{0.15}|1\rangle_c) \otimes |0, 0\rangle_p$  given by Eq. (4e), coin ( $\hat{H}$ ) and shift ( $\hat{S}$ ) operators given by Eqs. (5) and (6) respectively, and measurement operator  $\hat{M}_1$  (Eq. (7)). The thin line of (i) (red color online) shows the maximum degree of entanglement between walkers attainable in the post-measurement quantum state  $|\psi\rangle_{t,pm}^{c_1}$ , and the thick line of (i) (blue color online) shows the actual entanglement between walkers available at each step. We can see that the asymptotics of entanglement values given in plot (ii) tend to the same values as those shown in Fig. (13), obtained from a coin  $|0\rangle_c$  post-measurement state  $|\psi\rangle_{t,pm}^{c_0}$  computed from a quantum walk with the same initial state (Eq. (4e)).

of entanglement possible at each step (purely from the dimensionality of the space explored by the walkers in a given step) for either coin measurement outcome. Nevertheless, our simulations also show that the entanglement ratio (= entanglement generated/highest value of entanglement possible, for each step) tends to converge to a rather high value (for example, to 0.8 or 0.9), and the actual convergence value seems to depend on the coin initial state and on the coin measurement outcome.

Convergence of entanglement ratio leads to a most

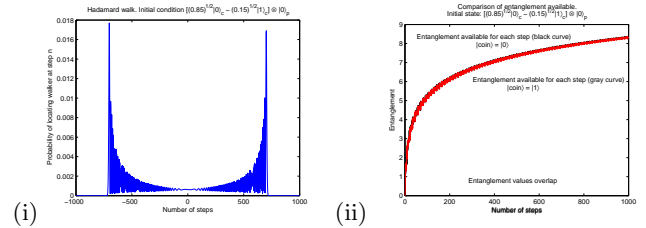


FIG. 15: Plot (i) presents the probability vs location graph of a 1000-step Hadamard quantum walk with an initial state  $(\sqrt{0.85}|0\rangle_c - \sqrt{0.15}|1\rangle_c) \otimes |0\rangle_p$  and shift operator provided by Eq. (11). The symmetry of the probability distribution shown in plot (i) is the same as that of a Hadamard quantum walk with initial state given by  $|\psi\rangle = (\sqrt{0.85}|0\rangle_c - \sqrt{0.15}|1\rangle_c) \otimes |0, 0\rangle_p$  and shift operator given by Eq. (6). In this case, the asymptotics of entanglement values for both coin post-measurement states  $|\psi\rangle_{t,pm}^{c_0}$  (black curve of plot (ii)) and  $|\psi\rangle_{t,pm}^{c_1}$  (gray curve of plot (ii)) tend to the same values.

interesting result: the actual value towards which the entanglement ratio converges, for each coin measurement outcome, depends on the symmetry of the coin initial state. However, the relationship is not straightforward, as it is possible to find two coin initial states  $(|\psi\rangle_0 = \frac{1}{\sqrt{2}}|0\rangle + \frac{i}{\sqrt{2}}|1\rangle)$  and  $(|\phi\rangle_0 = \sqrt{0.85}|0\rangle - \sqrt{0.15}|1\rangle)$  such that, although both produce balanced probability distributions, only one coin initial state ( $|\phi\rangle_0$ ) makes the asymptotical values of entanglement, for both coin measurements, converge to the same value. Going to two walkers and exploring their entanglement can thereby reveal differences in two quantum walks which are not differentiated easily in the usual case of a single walker.

A noteworthy feature of our algorithm is the high amount of the entanglement generated between the walkers which grows with the number of steps. Our scheme is particularly applicable in physical realizations where the coin is a qubit (such as an atom or a superconducting qubit) which interacts with a distinct physical system (such as an electromagnetic field mode) acting as a walker [11, 12, 30]. Taking two such walkers, each being a distinct system, one can probe how entanglement is generated between them through our algorithm. As such walkers do not naturally interact with each other, using the coin (qubit) system is the only way to entangle them. A recent circuit QED suggestion for the physical implementation of a quantum walk [30] even estimate a walk of a significant number of steps to be carried out within the decoherence times of the relevant physical systems. Simply enhancing such schemes to two walkers would enable observing the entanglement generation mechanism that we have presented and analyzed in this paper.

#### IV. ACKNOWLEDGEMENTS

S.V-A. gratefully acknowledges useful discussions with Dr J.L. Ball as well as the support of SNI, CONA-CyT and Tecnológico de Monterrey Campus Estado de

México. S.B. acknowledges the support of the EPSRC, UK, the QIP IRC (GR/S82176 /01), the Royal Society

and the Wolfson Foundation.

- 
- [1] S. Godoy and S. Fujita, A quantum random-walk model for tunneling diffusion in a 1D lattice, *J. Chem Phys.* **97**(7) (1992) 5148-5154.
- [2] S. P. Gudder, *Quantum probability* (Academic Press Inc., 1998)
- [3] N. Konno, Limit theorems and absorption problems for quantum random walks in one dimension, *Quantum Information and Computation* **2** (2002) 578-595.
- [4] R.P. Feynman, Quantum Mechanical Computers, *Foundations of Physics* **16**(6) (1986) 507-531.
- [5] B. A. Chase and A.J. Landhal, Universal quantum walks and adiabatic algorithms by 1D Hamiltonians, arXiv:0802.1207 (2008).
- [6] Y. Aharonov, L. Davidovich, and N. Zagury, Quantum random walks, *Phys. Rev. A* **48** (1993) 1687-1690.
- [7] U. Schöning, A probabilistic algorithm for K-SAT and constraint satisfaction problems, in *Proceedings of the 40<sup>th</sup> Annual Symposium on Foundations of Computer Science (FOCS)*, (IEEE, 1999), pp. 410-414.
- [8] K. Iwama and S. Tamaki, Improved upper bounds for 3-SAT, *Electronic Colloquium on Computational Complexity* **53** (2003).
- [9] R. Motwani and P. Raghavan, *Randomized Algorithms* (Cambridge University Press, 1995).
- [10] J. Du, H. Li, X. Xu, M. Shi, J. Wu, X. Zhou, and R. Han, Experimental implementation of the quantum random-walk algorithm, *Phys. Rev. A* **67** (2003) 042316.
- [11] B.C. Sanders, S.D. Bartlett, B. Tregenna, and P.L. Knight, Quantum quincunx in cavity quantum electrodynamics, *Phys. Rev. A* **67** (2003) 042305.
- [12] G. S. Agarwal and P. K. Pathak, Quantum random walk of the field in an externally driven cavity, *Phys. Rev. A* **72** (2005) 033815.
- [13] C. M. Chandrashekar, Implementing the one-dimensional quantum (Hadamard) walk using a Bose-Einstein condensate, *Phys. Rev. A* **74** (2006) 032307.
- [14] A. Rai, G. S. Agarwal, and J. H. H. Perk, Transport and quantum walk of nonclassical light in coupled waveguides, *Phys. Rev. A* **78** (2008) 042304.
- [15] S.E. Venegas-Andraca, *Quantum Walks for Computer Scientists* (Morgan and Claypool, 2008).
- [16] M. Mohseni, P. Rebentrost, S. Lloyd, and A. Aspuru-Guzik, Environment-assisted quantum walks in energy transfer of photosynthetic complexes, *J. Chem. Phys.* **129** (2008) 174106.
- [17] P.L. Knight, E. Roldán, and J.E. Sipe, Quantum walk on the line as an interference phenomenon, *Phys. Rev. A* **68** (2003) 020301.
- [18] P.L. Knight, E. Roldán, and J.E. Sipe, Optical cavity implementations of the quantum walk, *Optics Communications* **227** (2003) 147-157.
- [19] P.L. Knight, E. Roldán, and J.E. Sipe, Propagating quantum walks: the origin of interference structures, *J. Mod. Op.* **51**(12) (2004) 1761-1777.
- [20] I. Carneiro, M. Loo, X. Xu, M. Girerd, V. Kendon, and P.L. Knight, Entanglement in coined quantum walks on regular graphs, *New J. Phys.* **7** (2005) 156.
- [21] O. Maloyer and V. Kendon, Decoherence vs entanglement in coined quantum walks, *New J. Phys.* **9** (2007) 87.
- [22] G. Abal, R. Siri, A. Romanelli, and R. Donangelo, Quantum walk on the line: entanglement and non-local initial conditions, *Phys. Rev. A* **73** (2006) 042302.
- [23] G. Abal, R. Donangelo, and H. Fort, Long-time entanglement in the quantum walk, in *Annals of the 1st Workshop on Quantum Computation and Information 9-11 October 2006, Pelotas, RS, Brazil* (2007) pp. 189-200.
- [24] S.K. Goyal and C.M. Chandrashekar, Spatial entanglement in many body system using quantum walk, *quant-ph/Arxiv:0901.0671* (2009).
- [25] M. Annabestani, M.R. Abolhasani, and G. Abal, Asymptotic entanglement in a coherent 2D quantum walk, *quant-ph/Arxiv:0901.1188* (2009).
- [26] Y. Omar, N. Paunković, L. Sheridan, and S. Bose, Quantum Walk on a Line with Two Entangled Particles, *Phys. Rev. A* **74** (2006) 042304.
- [27] S.E. Venegas-Andraca, J.L. Ball, K. Burnett, and S. Bose, Quantum Walks with Entangled Coins, *New J. Phys.* **7** (2005) 221.
- [28] C. M. Chandrashekar, Discrete time quantum walk model for single and entangled particles to retain entanglement in coin space, *arXiv:quant-ph/0609113* (2006).
- [29] C. Liu and N. Petulant, One-dimensional quantum random walks with two entangled coins, *quant-ph/Arxiv:0807.2263* (2009).
- [30] P. Xue, B. C. Sanders, A. Blais, and K. Lalumiere, Quantum walks on circles in phase space via superconducting circuit quantum electrodynamics, *Phys. Rev. A* **78**, (2008) 042334.